2022

CFD Modeling Of Very High Air Flow In A Residential Clothes Dryer To Investigate Pressure Loss And Flow Through The Air Flow Path

Christopher Lawrence Hall

Steve Karman

Philip Boudreaux

Viral Patel

Dean Ellis

See next page for additional authors

CFD Modeling of Very High Air Flow In A Residential Clothes Dryer To Investigate Pressure Loss And Flow Through The Air Flow Path

Christopher HALL[1]*, Steve KARMAN[1], Philip BOUDREAUX[2], Viral PATEL[2], Dean ELLIS[1], Kyle GLUESENKAMP[2], Anthony GEHL[2]

[1]Computational Sciences and Engineering Division
[2]Buildings and Transportation Science Division
Oak Ridge National Laboratory
Oak Ridge, TN, USA
hallcl@ornl.gov
* Corresponding Author

ABSTRACT

Thermoelectric heated residential clothes dryers have previously been shown to be capable of up to 85% greater energy efficiency than typical electric resistance heated clothes dryers. However, added air flow resistance through the thermoelectric heat sinks can significantly reduce the overall efficiency of the dryer. Minimizing air flow resistance in the existing dryer air flow path may offset some of the added resistance from the thermoelectric heat sinks. A three-dimensional computational fluid dynamics model was developed of a conventional clothes dryer to investigate pressure loss and flow through the dryer. The model was validated to laboratory data and used to predict dryer performance at very high air flow rates (up to 0.142 m^3/s (300 cubic feet per minute)). The model was used to examine modified geometric configurations to reduce pressure loss throughout the system and increase efficiency of the clothes dryer. Modeling results showed that enlarging the rear duct by 20% could reduce pressure loss through the dryer by up to 20%.

1. INTRODUCTION

Clothes dryers account for a significant percentage of household energy usage, up to 5% (US Energy Information Administration, 2019). Reducing the energy usage of a household clothes dryer can therefore have a large impact on overall energy usage. Previous studies have shown that a thermoelectric heat pump-based clothes dryer can produce significant improvements in energy efficiency of up to 85% (Patel *et al*, 2018; Patel *et al*, 2020). However, these experiments have also shown a significant increase in drying time.

To reduce the drying time, one potential option is to increase the air flow from a typical clothes dryer. In order to maintain efficiency at these higher flow rates, pressure loss through the system needs to be minimized. The objective in the current study is to use computational fluid dynamics (CFD) modeling to find areas of large pressure loss and find possibilities to reduce this pressure loss at higher flow rates.

2. MODELING METHODOLOGY

2.1 Initial CAD Model and Mesh

To develop a three-dimensional CFD model of a household clothes dryer, the internal geometry of the air flow path must be discretized before being imported into a modeling program. A computer-aided design (CAD) model of the dryer was developed prior to developing the CFD model.

A commercially available dryer was disassembled, the dimensions of the individual components were measured and input into SolidWorks, a CAD program (SOLIDWORKS, 2022). The individual pieces were then linked together within the SolidWorks to get the total internal geometry of the air flow path, from the inlet at the electric resistance heater through the drum to the outlet at the back of the dryer. Other significant flow restrictions were also measured and added into the CAD model including the heater coils, the grate at the rear of the drum, and the front grate (where the lint filter is installed). These represent significant areas of flow restrictions and geometry changes, where pressure

losses are expected to be significant. Figure 1 shows a translucent overview of the CAD geometry, with the inlet, heater coils, rear grate, and front grate labeled.

Once the CAD model was complete, it was imported into the Pointwise (Cadence, 2022) meshing software package to create a three-dimensional mesh. The Pointwise meshing software allowed for finer control of the boundary layers and mesh setup through the complicated geometry. This mesh was then imported into the Ansys Fluent 17.2 modeling software package (Ansys, 2022). Ansys Fluent is a well-regarded commercial code that has been used successfully for many CFD studies, recently by Tancabel *et al* (2021) and Sarkar (2021). Figure 2 shows the mesh cross section from the middle of the dryer drum, with an emphasis on the mesh sizing at the boundary layer.

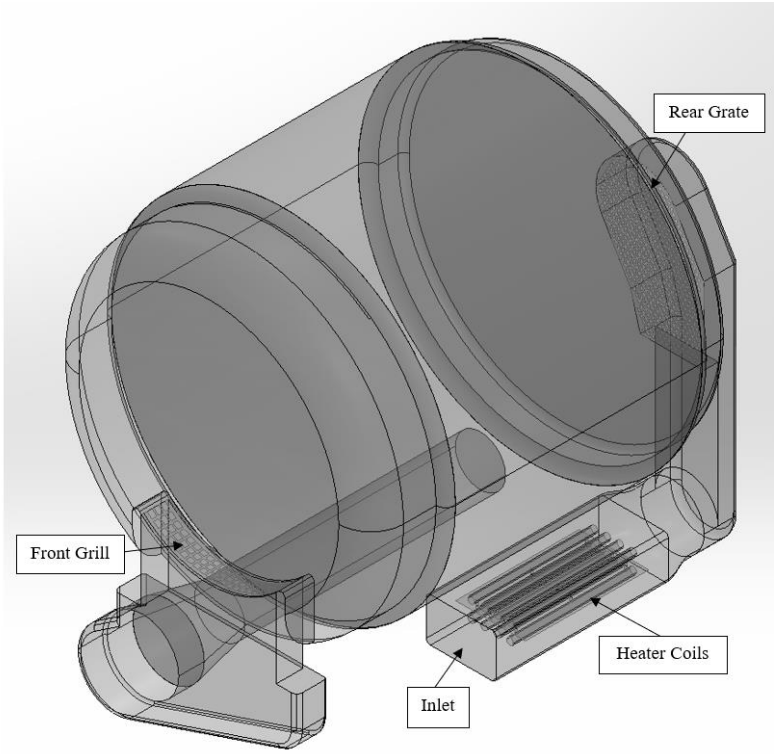

Figure 1: CAD model of clothes dryer with selected points labeled

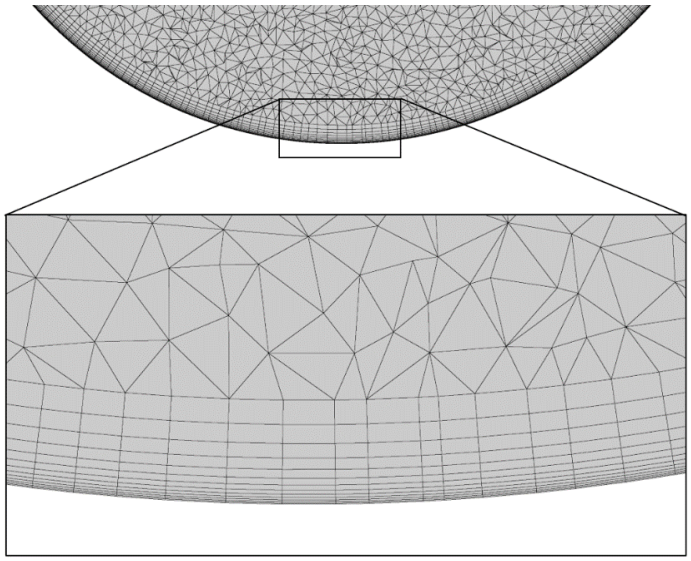

Figure 2: Clothes dryer drum mesh cross section from PointWise

2.2 CFD Model Assumptions

Two significant assumptions were included in the CFD model of the clothes dryer. First, the air flow within the model was assumed to be incompressible. In support of this assumption, velocities values were calculated within the domain to check for compressibility effects. From the measurements taken during the development of the CAD model, the rear duct had one of the smallest cross-sectional areas within the air flow path, with a measured cross-sectional area of 0.005 m^2. Based on the typical flow rate measured during experiments of 0.078 m^3/s (165 ft^3/min), this produced an average velocity in the section of 15.4 m/s. For room temperature air, this gives a Mach number of 0.05, well under the 0.3 value that is commonly treated as the limit where compressibility effects become important (Oosthuizen *et al*, 1997). Based on this, even at twice the flow rate, the flow can be considered incompressible and modeled as such. This approach has been used in similar studies in the past (Rezk *et al*, 2011; Ramachandran *et al*, 2018).

The second significant assumption was that heat transfer was disregarded in the model. As the objective of the model was to investigate locations of large pressure loss and not attempt to increase heat transfer efficiency, including heat transfer would have added unnecessary complexity and increased model run times.

3. CFD MODEL VALIDATION

3.1 Experimental Summary

An experimental effort was undertaken to measure the pressure losses through the clothes dryer to incorporate into the CFD model validation. These experiments involved the installation of pressure taps connected to Setra Model-264 differential pressure transducers at locations throughout the dryer. The dryer was then run for typical operating conditions, and pressure measurements were recorded from each pressure tap. Experiments with the heating elements disabled and no clothing material in the dryer were run to develop baseline conditions for model validation. Total air flow at the exhaust of the dryer was measured using a Veltron traversing pitot station. Figure 3 shows the locations of the pressure taps, and Figure 4 shows two of the pressure taps installed in the dryer at the rear duct. The data from the pressure taps were recorded via LabView software on a computer (National Instruments, 2022), and the results are presented in Table 1.

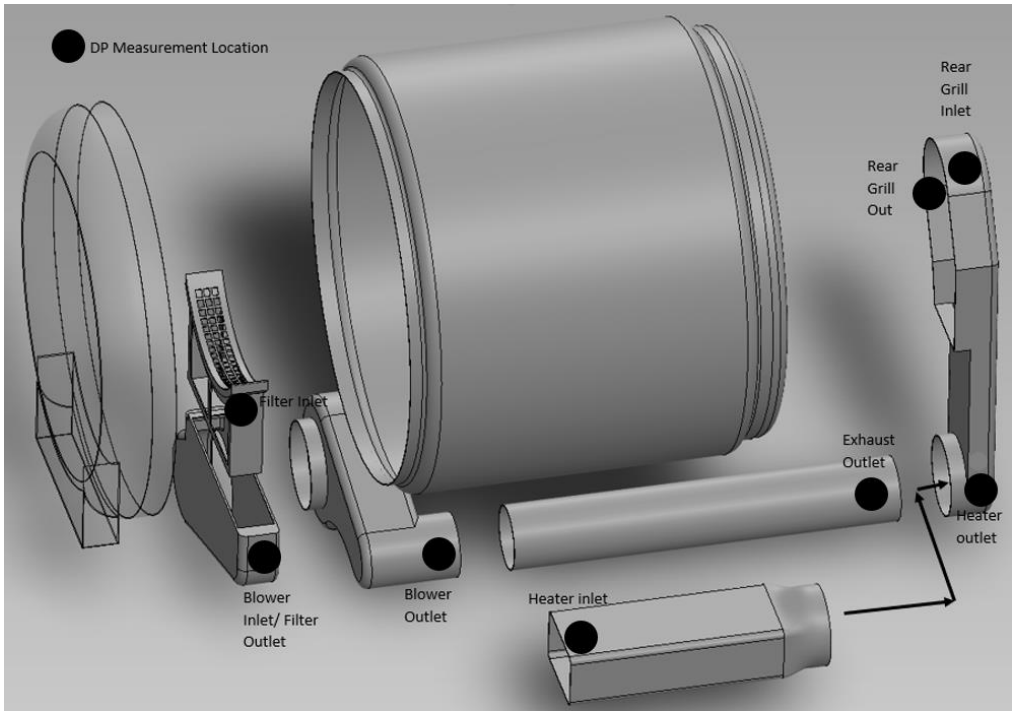

Figure 3: Pressure tap locations within the dryer

Figure 4: Photo of the rear duct, showing the locations of the two pressure taps for the Rear Grill Inlet and Rear Grill Out

Table 1: Pressure measurements along dryer air flow path at a flow rate of 0.078 m^3/s

Measurement Location	Differential Pressure (With respect to ambient) [Pa]
Heater Inlet	-25.9
Heater Out	-62.5
Rear Grill Inlet	-37.6
Rear Grill Out	-51.3
Filter Inlet	-85.4
Blower Inlet/Filter Out	-152.3
Blower Outlet	174.9
Exhaust Outlet	83.1

Based on previous dryer experiments, air leakage along the air flow path was expected. Additional experiments were run with various sections of the dryer isolated to parameterize the air flow leakage rates per section. Table 2 gives the air leakage values by dryer section at typical flow rates.

Table 2: Leakage rates at the various dryer sections at a flow rate of 0.078 m3/s

Dryer Section	Average Pressure Differential [Pa]	Leakage Flow [m^3/s]	Leak Direction	Percent of Operational Flow
Inlet to Rear Grill	-31.7	0.0086	Inflow	11%
Rear Grill to Front Grill (rotating seals)	-71.7	0.0056	Inflow	7%
Front Grill to Blower Inlet	-157.8	0.0068	Inflow	9%
Blower Inlet to Exhaust	129.0	0.0038	Outflow	5%

3.2 Model Initialization

The model was set up using the shear stress transport (SST) k-ω turbulence model option in Fluent with the fluid set as air (ρ=1.225 kg/m3, μ=1.7894E-05 kg/m-s). Pressure boundary conditions were set at the inlet and outlet based on the experimentally observed values. The blower fan was modeled as a pressure jump boundary condition within Fluent. To simulate the experimentally observed air leakages, mass-flow inlet boundary conditions were specified at

leakage locations around the mesh. The model was run with steady-state conditions until the model had converged, and simulated pressures at the inlet and outlet had stabilized. A mesh sensitivity study was undertaken, and a final mesh size of 11 million cells was selected for the modeling effort. Figure 5 shows geometry with the leakage areas highlighted and labeled around the mesh.

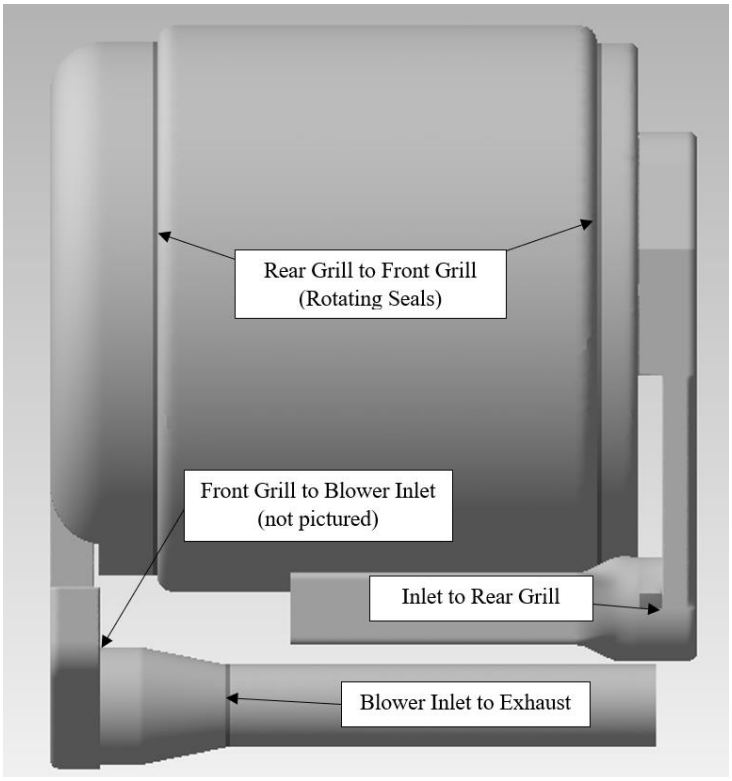

Figure 5: Dryer model domain with leakage locations

3.3 Model Validation Results

For validation of the model to the experimental results, the principal areas of adjustment within the model were the value of the pressure jump boundary condition and distribution of the leakage values. Distribution of the leakage value through the rotating seals around the drum was set to 50% at each seal. The pressure jump boundary condition was iterated until the modeled pressures matched acceptably with the observed pressures. Table 3 gives the measured and simulated pressures through the dryer, and Figure 6 shows the same data graphically.

Table 3: Model validation results for pressure at a flow rate 0.078 m^3/s

Location	Experimental Pressure [Pa]	Model Simulated Pressure [Pa]	Relative Error
Inlet	-25.9	-6.4	75%
Rear Grill In	-37.6	-59.3	58%
Blower Inlet	-152.3	-213.0	40%
Blower Out	174.9	159.2	9%
Exhaust	83.1	83.0	0%

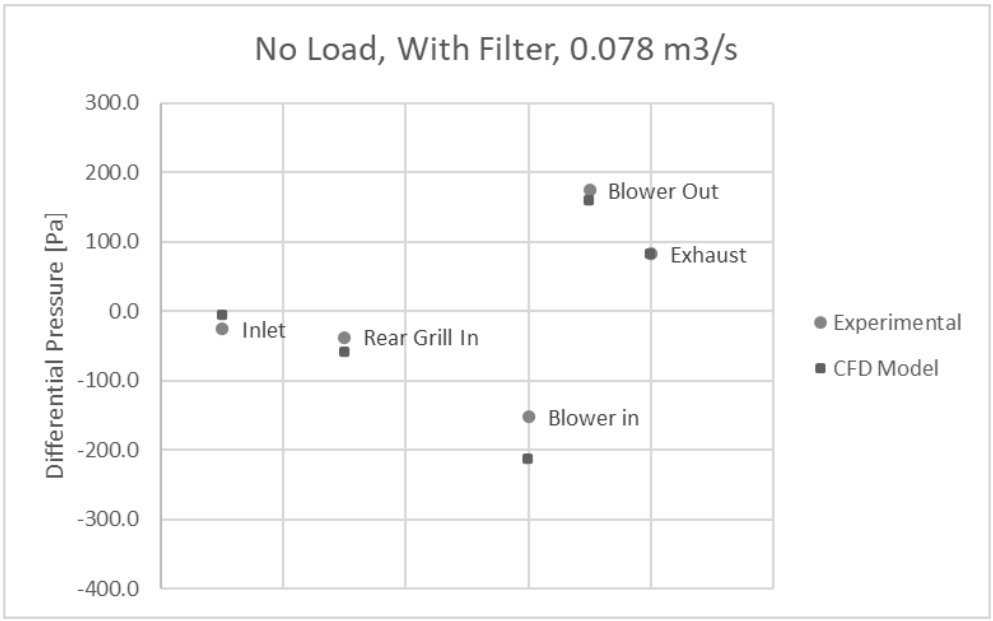

Figure 6: Model and experimental pressure results at a flow rate of 0.078 m^3/s

3.4 Validation at Higher Flow Rates

The model was then extended to simulate the effects of higher air flow rates with the external fan. Within the dryer, the internal blower fan was removed, and the larger blower was attached to the exhaust duct outside of the dryer shell. The model was modified to represent this set up, with no outflow leaks and no pressure jump boundary condition. The model was set to mass inflow boundary conditions at the inlet and leakage locations, and an outflow boundary condition at the outlet. Leakage values were scaled linearly at each location with the overall flow rate. Total air flow rates at the outlet of 0.078, 0.094, 0.118, and 0.142 m^3/s (165, 200, 250, 300 cubic feet per minute (CFM)) were run with the updated boundary conditions. Table 4 gives the boundary conditions for the higher flow rates.

Table 4: Boundary conditions for high flow rates

Boundary Condition Location	**Flow Direction**	**Flow Rate (m^3/s)**			
		0.078 m^3/s	**0.094 m^3/s**	**0.118 m^3/s**	**0.142 m^3/s**
Inlet	Inlet	0.053	0.064	0.080	0.097
Rear Grill In	Inlet	0.009	0.010	0.013	0.016
Blower Inlet	Inlet	0.006	0.007	0.008	0.010
Blower Out	Inlet	0.007	0.008	0.010	0.012
Exhaust	Inlet	0.004	0.005	0.006	0.007
Outlet	Outlet	0.078	0.094	0.118	0.142

The models were run for the various boundary conditions, and total pressure loss through the dryer was calculated. Total pressure loss through the physical dryer was measured in the lab with the same pressure tap setup as in the validation portion. Table 5 and Figure 7 show the model results compared to the experimental values. As can be seen, the model reasonably matches the experimental total pressure loss with the flow rates up to 0.142 m^3/s.

Table 5: High flow model pressure results compared to experimental results

Flow Rate (m^3/s)	**Experimental Pressure Drop over Dryer [Pa]**	**Model Simulated Pressure Drop [Pa]**	**Relative Error**
0.078	470.1	408.1	13%
0.094	658.3	613.1	7%
0.118	977.4	956.4	2%
0.142	1355.6	1381.8	2%

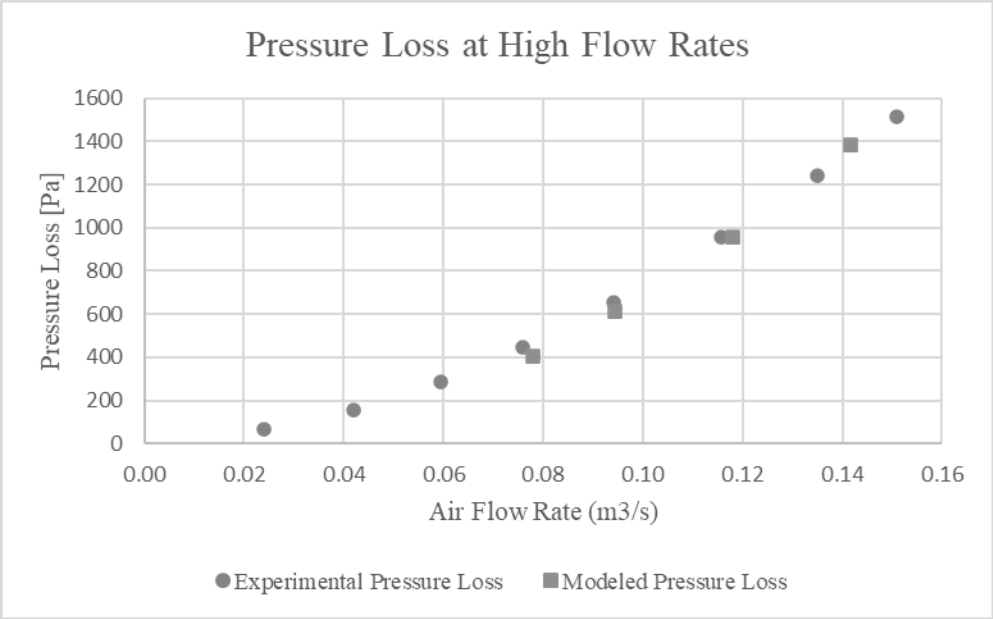

Figure 7: Model and experimental pressure loss through the dryer at high flow rates

4. MODEL DRIVEN DESIGN OPTIMIZATION AND RESULTS

Once the model was validated to flow rates up to 0.142 m^3/s, it was used to investigate potential areas of geometric modifications to reduce pressure loss through the dryer. Examinations of simulated pressures and velocities for all flow rates revealed several areas of potential geometric modifications. However, modifications were limited to the constraints of the existing shell of the dryer. Additionally, large areas of flow restriction such as the lint filter and rear grate had to remain unchanged to maintain dryer function. Based on these limitations and the output from the model runs, the rear duct of the dryer was selected as the principal area of modification to improve dryer performance. This area showed high velocities, large pressure changes, and could be modified to stay within the dryer shell.

4.1 Modification Cycle

To investigate the impacts from various modifications, a modeling cycle was applied that consisted of modifying the CAD geometry for the rear duct, remeshing the rear duct and appending it to the existing mesh, running the model with air flowrates from 0.078 to 0.142 m^3/s, and examining the results for both pressure loss and flow changes. Based on the results, a new design was developed, and the modeling cycle was repeated for the new design.

4.2 Rear Duct Modifications

Modification 1 involved smoothing the transitions of the rear duct where it interfaced with the heating element and the rear grate. The radius of the rounding at the rear of the duct was increased with a goal to smooth the air flow and reduce drag. Figure 8 (b) shows the geometry for Modification 1.

Modification 2 involved smoothing the transitions of the rear duct where it interfaced with the heating element and the rear grate. The radius of the rear duct was left the same as the initial rear duct. Figure 8 (c) shows the geometry for Modification 2.

Modification 3 was based on Modification 2, with an increase in the cross-sectional area of the duct. Figure 8 (d) shows the geometry for Modification 3. The goal of this modification was to reduce velocity and therefore decrease the drag force in accordance with equation (1).

$$D = C_d \rho A (V^2/2) \quad (1)$$

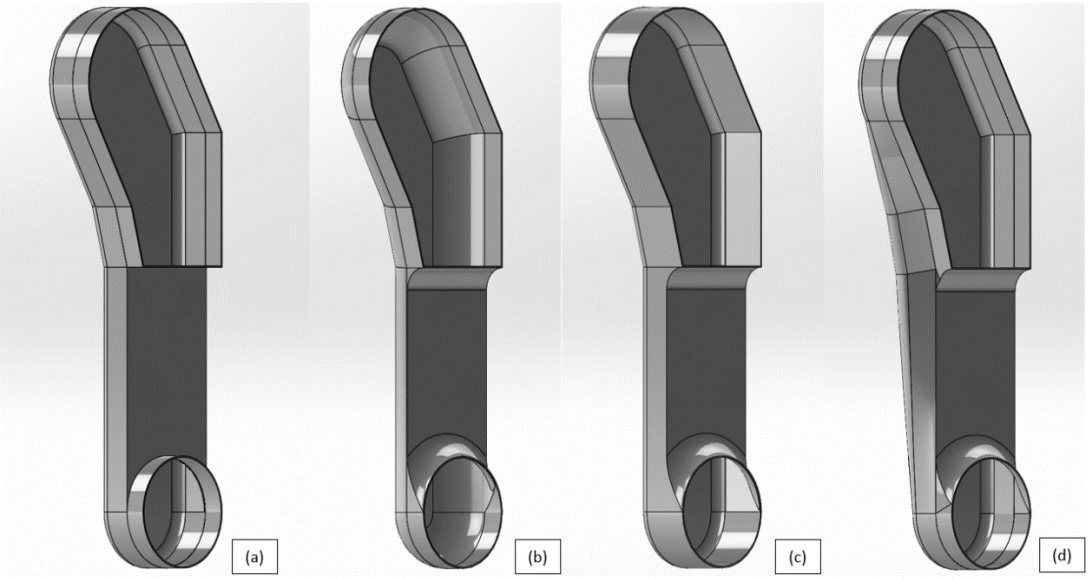

Figure 8: Rear duct modifications tested for pressure loss through the dryer - (a) base rear duct, (b) Modification 1, (c) Modification 2, (d) Modification 3

4.3 Model Results Discussion

Table 6 presents the model simulated pressure loss over the clothes dryer for the three modifications tested. As seen in the table, Modification 1 decreased the cross-sectional area of the duct and increased the overall pressure loss through the dryer. Modification 2 kept the same duct cross section with the smoothed inlet and outlet transitions. The smoothed transitions did reduce the overall pressure loss through the dryer at all flow rates. Modification 3 increased the cross-sectional area in the duct with an additional improvement in the overall pressure loss through the dryer when compared to Modification 2.

Figure 9 shows the flow paths colored by velocity magnitude, with the rear duct circled with a dashed line for emphasis. The orientation of this figure is the same as in Figure 5. Velocity results were compared to the base duct (Figure 9 (a)). As can be seen, Modification 1 increased velocity in the rear duct (Figure 9 (b)) compared to the base rear duct as shown by the brighter colored lines in the rear duct. Modification 2 (Figure 9 (c)) reduced velocity compared to the base duct and Modification 1. Modification 3 (Figure 9 (d)) reduced velocity in the rear duct compared to the base duct and the other modifications. Lower velocities in the rear duct are associated with lower total pressure loss over the dryer, as seen in Table 6.

This relationship is also supported using equation (2a), the one-dimensional conservation of momentum equation (Bernoulli's equation), rearranged to equation (2b):

$$p_1+\rho V_1^2/2 = p_2+\rho V_2^2/2 \quad (2a)$$

$$p_1-p_2 = \rho(V_2^2-V_1^2)/2 \quad (2b)$$

Applying equation (2b) to the dryer, point 1 is assumed to be at the bottom of the rear duct and point 2 is assumed to be at the midpoint of the rear duct (the higher velocity region). As V_2 increases compared to the base duct (as occurs in Modification 1), (p_1-p_2) must increase compared to (p_1-p_2) for the base duct. This leads to a larger pressure change over the rear duct. If V_2 decreases compared to the base duct (as occurs with Modification 3), (p_1-p_2) decreases compared to (p_1-p_2) for the base rear duct, leading to a lower pressure loss over the rear duct. As the remainder of the dryer is unchanged, this leads to larger total pressure loss for Modification 1 and a smaller total pressure loss for Modification 3, in agreement with the model results shown in Table 6. In general, larger cross-sectional areas will yield lower velocities, which is supported by the data in Table 6, where the largest improvement in total pressure loss is from the duct modification with the largest area.

Table 6: Pressure loss values for the rear duct modifications compared to the base pressure loss

Rear Duct Modification	Cross Sectional Area (cm^2)	Flowrate (m^3/s)	Total Pressure Loss (Pa)	Difference From Base Run
Base	50.6	0.078	408.1	--
		0.094	613.1	--
		0.118	956.4	--
		0.142	1381.8	--
Modification 1	48.4	0.078	425.5	4%
		0.094	641.5	5%
		0.118	975.0	2%
		0.142	1456.0	5%
Modification 2	50.6	0.078	350.6	-14%
		0.094	530.3	-13%
		0.118	817.1	-15%
		0.142	1167.6	-16%
Modification 3	61.5	0.078	333.0	-18%
		0.094	497.5	-19%
		0.118	779.8	-18%
		0.142	1107.0	-20%

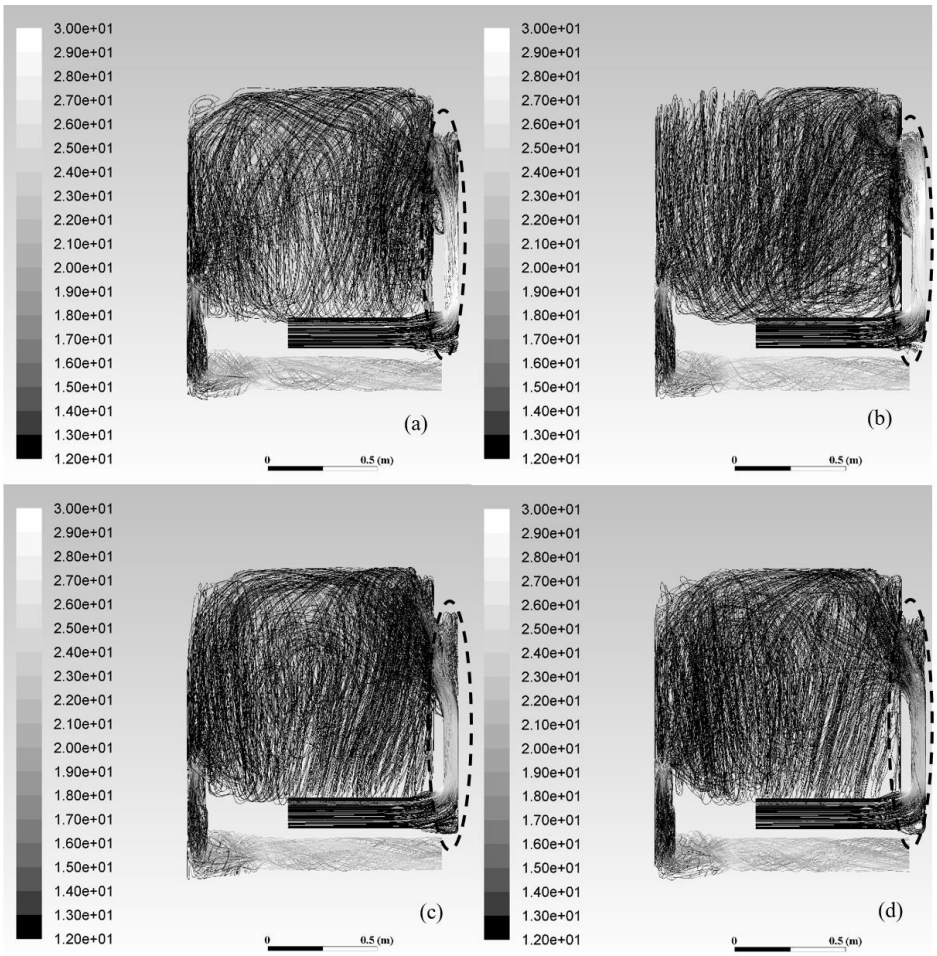

Figure 9: Velocity magnitudes (m/s) along the dryer air flow path for each of the rear duct modifications – (a) base rear duct, (b) Modification 1, (c) Modification 2, (d) Modification 3

5. CONCLUSIONS

A CFD model was developed of a household clothes dryer and was validated to experimentally measured pressures at air flow rates from 0.078 to 0.142 m^3/s (165 to 300 CFM). The validated CFD model was used to test various rear duct designs to predict changes in pressure loss through the dryer. An optimized design of the rear duct was developed that increased the cross-sectional area of the rear duct by nearly 20% combined with the addition of smoothed flow transitions. The optimized geometry produced an improvement in pressure loss of nearly 20% at all air flow rates tested. This should also result in lower blower work to produce the higher air flow rates, leading to further increased efficiency of the dryer.

NOMENCLATURE

A	area	(m^2)
CAD	Computer Aided Design	(-)
C_d	drag coefficient	(-)
CFD	Computational Fluid Dynamics	(-)
CFM	cubic feet per min	(ft^3/min)
D	drag force	(N)
V	velocity	(m/s)
p	pressure	(Pa)
ρ	density	(kg/m^3)
μ	viscosity	(kg/m-s)

REFERENCES

Ansys. (2022). Fluent. https://www.ansys.com/products/fluids/ansys-fluent

Cadence. (2022). Pointwise. https://www.pointwise.com/

National Instruments. (2022). LabVIEW. https://www.ni.com/en-us/shop/labview.html

Oosthuizen, P. H. & Carscallen, W. (1997). *Compressible Fluid Flow*.

Patel, V. K., Boudreaux, P. R., & Gluesenkamp, K. R. (2020). "Validated model of a thermoelectric heat pump clothes dryer using secondary pumped loops," *Applied Thermal Engineering*. *184 (1)*.

Patel, V., Gluesenkamp, K., Goodman, D., & Gehl, A. (2018). Experimental evaluation and thermodynamic system modeling of thermoelectric heat pump clothes dryer. *Applied Energy. 217*. 221-232.

Ramachandran, R., Akbarzadeh, M., Paliwal, J., & Cenkowski, Stefan. (2018). Computational Fluid Dynamics in Drying Process Modelling—a Technical Review. *Food and Bioprocess Technology*. *11*. 271-292

Rezk, Kamal & Forsberg, Jan. (2011). Geometry development of the internal duct system of a heat pump tumble dryer based on fluid mechanic parameters from a CFD software. *Applied Energy*. *88*. 1596-1605.

Sarkar, S. (2021) "Computational Fluid Dynamics (CFD) Modeling of Two Phase Refrigerant Flow in Evaporator Refrigerant Distribution System". International Refrigeration and Air Conditioning Conference. Paper 2267.

SOLIDWORKS. (2022). 3D mechanical CAD. https://www.solidworks.com/

Tancabel, J., Gerstler, W., Erno, D., Ling, J., Aute, V., De Bock, H. P. J., and Radermacher, R. (2021) "CFD-based Analysis & Correlation Development for a Novel Multi-furcating Heat Exchanger for High Temperature, High Pressure Applications". International Refrigeration and Air Conditioning Conference. Paper 2154.

US Energy Information Administration. (2019). Use of energy explained – energy use in homes. (2019). Retrieved April 13, 2022, from https://www.eia.gov/energyexplained/use-of-energy/electricity-use-in-homes.php

ACKNOWLEDGEMENT

This manuscript has been authored by UT-Battelle, LLC, under contract DE-AC05-00OR22725 with the US Department of Energy (DOE). The publisher acknowledges the US government license to provide public access under the DOE Public Access Plan (http://energy.gov/downloads/doe-public-access-plan). This research used resources at the Building Technologies Research and Integration Center, a DOE Office of Science User Facility operated by the Oak Ridge National Laboratory. The authors would also like to acknowledge Dr. Wyatt Merrill, Technology Manager – Building Electric Appliances, Devices and Systems, U.S. Department of Energy Building Technologies Office.